Aerothermodynamic analysis of an intercooler

Guilherme Gomes dos Santos
guilherme.g.santos@tecnico.ulisboa.pt

Instituto Superior Técnico, Universidade de Lisboa, Portugal

february 2021

Abstract

Heat exchangers are components with applications in various industries and everyday equipment. Currently, the market trend is focused on obtaining compact high-performance heat exchangers. One of the existing models is the *intercooler* which function is cooling the engine intake gases. The performance of this component has a direct influence on the performance of the engine, the better the performance of the *intercooler*, the better is the overall performance of the car. Following this line of thought, together with JDeus, we optimized the performance of a *intercooler* already studied and currently in production by JDeus. The objective was to obtain the best possible performance without changing the volume of the component. The study was fulfilled in a multi-scale context. A macroscopic scale, where the results of the optimization were tested in a 3D simulation of the entire *intercooler*. A mesoscopic scale, where a representative section was studied, in order to have a perspective on the performance of the entire component. And a microscopic scale, where we characterized the fins used for various heights to be able to use them during the optimization. The optimization process was carried out using a genetic algorithm and was divided into 3 types: optimization without fins, optimization with fins, and optimization in volume with and without fins. The results obtained were validated by comparing the 3D simulation with experimental results provided by JDeus.
Keywords:*intercooler*, genetic algorithm, multi-scale, optimization, CFD

1. Introduction

Heat exchangers are components with several applications throughout many industries. These equipment purpose is to exchange heat between two fluids, one hot and the other cold. An *intercooler* is a heat exchangers that is used to cool the engine intake gases, after their passage in the turbo-compressor. The improvement of these components performance is crucial not only for a good vehicle performance, theme studied by Canli *et al*. [3], but also for a good energetic recovery and volume reduction of the equipment. The *intercooler* also affects the emission of polluting gases as studied by Lin *et al*. [9].

The heat exchangers, in order to improve their performance in exchanging, are suited with fins, components that increase the heat exchanging area and promote turbulence and flow renovation near the wall. This increase in efficiency allows the *intercooler* to have a smaller volume, making it possible to other engine equipment increase their size and consequently their performance.

The theme of this dissertation was proposed by JDeus, a Portuguese company specialized in the research and development of heat exchangers for cars. This company is the main supplier for car brands like Toyota, as it belongs to the Denso group, a Japanese multinational company.

The thesis objectives were to improve the performance of an actual *intercooler* already developed by JDeus and in production. This optimization was focused in changing the fluid channels layout, increasing the number of channels and changing the height of each channel, in order to increase the thermal effectiveness without increasing the pressure drop in both fluids.

The study was performed using a CFD software ($STAR-CCM+$) and an optimization toolbox present in $MATLAB$. The optimization tool used was the Genetic Algorithm, optimization tool derived of the natural selection present in the nature. The two softwares were linked by the ability of $MATLAB$ of performing system commands. The $STAR-CCM+$ was initialized by the $MATLAB$ using the batch mode (session is started without opening a window) and a macro is read. The $MATLAB$ generates a script with the commands to scale the mesh to heights given by the Genetic Algorithm. Thus, the process of optimization was automatic, without the presence of the user.

The way this optimization was conducted differs from the usual optimizations present in the litera-

ture (Ismail 2018 [12]) [11] by not using the $LMTD$ and $NTU - \epsilon$ to analyze the performance. This optimization was exclusively done by numerical simulation, applying the porous media approach to simulate the presence of the fins, since simulating the fins is extremely expensive in computational power.

2. Theoretical background

2.1. Internal Flow

The flow inside a heat exchanger can be modeled as an internal flow, since the flow occurs inside a channel. The equations that rule the flow inside a channel are the *Hagen-Poiseulle* [10] for laminar flow (1):

$$u(y) = -\frac{dp}{dx}\frac{h^2}{2\mu}\left(1 - \frac{y^2}{h^2}\right) \tag{1}$$

For turbulent flow, an approximation of the $log - law$ (2) is used, with the parameters κ varying between 0.33-0.43 and B between 3.5-6.1, depending on the Re_d, according to Bailey *et al*. [2].

$$\frac{u(y)}{u_\tau} \approx -\frac{1}{\kappa}\ln\frac{yu_\tau}{\nu} + B \tag{2}$$

The heat transfer inside a channel is based on correlations. For laminar flow, the heat transfer is constant and based on the heating condition and the channel shape. For an infinite width channel with UWT, the N_u is 7.54. For turbulent flow, there is several correlations based on the flow Re_{D_h} and P_r (Dittus-Boelter [4]), and also on the flow friction factor (Gnielinski [5]).

Dittus-Boelter [4]

$$Nu_D = 0.023 Re_D^{\frac{4}{5}} Pr^n \tag{3}$$

Gnielinski [5]

$$Nu_D = \frac{f/8(Re_D - 1000)Pr}{1 + 12.7(f/8)^{\frac{1}{2}}(Pr^{\frac{2}{3}} - 1)} \tag{4}$$

2.2. Heat exchanger

The $LMTD$ and $NTU - \epsilon$ are two methods that allows the analysis of an heat exchanger. The $LMTD$ is based on the overall heat transfer equation ($q = UA\Delta T_{lm}$) using the Log Mean Temperature difference and knowing the overall thermal resistance between fluids. The $NTU - \epsilon$ is based on the effectiveness, type and configuration of the heat exchanger.

Counter-flow

$$\epsilon = \frac{1 - \exp -NTU[1 + (C_{min}/C_{max})]}{1 - (C_{min}/C_{max})\exp -NTU[1 + (C_{min}/C_{max})]} \tag{5}$$

2.3. Genetic algorithm

The tool used for optimize the *intercooler* performance was the Genetic Algorithm. This optimization algorithm is based on the natural selection and genetic crossover that happens on the nature. The variables that are chosen to be optimized are treated as genes, and a set of genes is an individual. The genes can be combined, a process called crossover that occurs when two individuals combine and create a new individual, with a genetic pool that contains genes from both parents. Also, a mutation can occur and change the genetic pool of and individual without predecessors having that characteristic. The last process that can occur is selection, that is when an individual passes his whole genetic pool to an individual of the new generation. The survival of an individual is evaluated by the fitness function or by discrete values, being the smaller the better. At the final generation the best individuals, the ones with the best survival rate, are chosen and represent the optimal values. If the optimization is a single objective, there is only one optimal point. If it has two or three variables to optimize, the optimal values are sorted in a Pareto curve or surface.

3. Methodology

The work was developed in a multi-scale approach, where we can identify three scales. A macroscale, where the whole *intercooler* was studied and simulated. This study allowed to verify and validate the models used during the optimizations, and also to obtain more significant data regarding the true performance of the *intercooler*. A mesoscale, where the REV of the *intercooler* was studied in order to obtain the global performance of the *intercooler* in a simpler and quicker way. This scale allowed to initiate the optimization process, since the model was basic enough to create a macro that modified the parameters of the REV in an automatic way. The last scale is a microscale where the fins properties were characterized in order to use the thermal non-equilibrium model present in the porous media model.

Firstly, the models and meshes that were going to be used throughout the entire work needed to be validated. For this study, the REV was used and the models (flow and thermal models) were validated comparing the results with correlations. With the models and meshes ready to begin the study of the *intercooler*, a script that connected the genetic algorithm with the STAR-CCM+ was developed. This script set the optimization process in an automatic way reading the data delivered by the genetic algorithm, and changing the mesh and boundary conditions according to the data received. This process allowed a quick way of performing several simulations without the presence of the user. The optimization was carried out in three ways. An optimization without fins (porous media not present), a optimization with fins (porous media present) and a volume optimization, where the total volume of

the core was reduced. The transition between the optimization without fins to the optimization with fins was possible due to the microscale study performed, that enable us to apply the thermal non-equilibrium method to the optimization process. In the end, the results from the optimization with fins were validated using the macroscale approach.

3.1. Porous media model

The porous media model replaces the fin with a *momentum* sink in the Navier-Stokes equations. This model allows the mesh to be more coarse since the real geometry of the fin is not present. The porosity $\chi = \frac{V_{fluid}}{V}$ is a crucial parameter that indicates the volume ratio between the total and fluid volume present in the media. The resistance of the fin is calculated using the Darcy-Forcheimer law.

$$\frac{\Delta P}{L} = \frac{\mu}{K_v} v_i + \frac{\rho}{K_i} v_i |v_i| \tag{6}$$

The K_v and the K_i are the resistance coefficients characteristic of the fin.

The energy model used was the thermal non-equilibrium, that solves an energy equation for each phase (solid and liquid).

Thermal Non-Equilibrium Model

$$\begin{aligned} &\frac{\partial(\chi\rho_{fluid}E_{fluid})}{\partial t} + \nabla\cdot(\chi\rho_{fluid}H_{fluid}\mathbf{v}) = \\ &-\nabla\cdot(\chi q_{fluid}) + \nabla\cdot(\chi\mathbf{T}\cdot\mathbf{v}) + Ah_t(T_{fluid} - T_{solid}) \\ &\frac{\partial((1-\chi)\rho_{solid}E_{solid})}{\partial t} = \\ &-\nabla\cdot((1-\chi)q_{solid}) + ah(T_{solid} - T_{fluid}) \end{aligned} \tag{7}$$

This model requires the input of the convection coefficient between the phases and the interaction area.

4. Results & discussion

4.1. Optimization without porous media

As the information regarding fins properties wasn´t available and correlations present in the literature (Kim *et al.* [7][8]) didn't match the results from JDeus, an optimization without the presence of fins was done just to obtain the trend between the channels heights and number of channels.

A 2D model of the REV was used, since the differences to a 3D model were minimal. The mesh independence is in table 1 and the select mesh was the one with 5.92×10^5 cells. The 2D model is a section of the 3D model.

Other simplification done was assuming a pure counter-flow heat exchanger, that is different from the reality. In the real *intercooler* the water go into the channel by the side and then turns to go along it. The table 2 shows the comparison between the real geometry and the simplified geometry.

The *intercooler* has 3 operating conditions and the solution has to maintain the performance in all three operating conditions. To clarify, if the solution is consistent in all three conditions, 27 different geometries were simulated in two operating conditions (low and very high). This study allowed to understand if an optimal solution in the very high operating condition is still an optimal solution.

Table 1: Mesh independence for 3D geometry of the REV

Nº off cells	$\Delta\mathbf{P_{air}}(\mathbf{Pa})$	Difference ($\Delta\mathbf{P_{air}}(\mathbf{Pa})$)
2.84×10^5	46.87	-15.8
3.44×10^5	46.87	-15.8
3.92×10^5	44.47	-9.9
4.90×10^5	44.45	-9.8
5.19×10^5	45.11	-11.4
5.92×10^5	41.61	-2.8
6.46×10^5	39.34	2.8
7.37×10^5	41.48	-2.5
9.65×10^5	38.51	4.9
1.14×10^5	40.48	-

Table 2: Comparison between the real geometry and a pure counter-flow geometry

	$\epsilon(\%)$	$\Delta\mathbf{P_{air}}(\mathbf{Pa})$	$\Delta\mathbf{P_{water}}(\mathbf{Pa})$
3D pure counter-flow	92.02	57.07	130.92
3D Real	89.71	57.92	135.39
Experimental	97.7	56.9	134.5

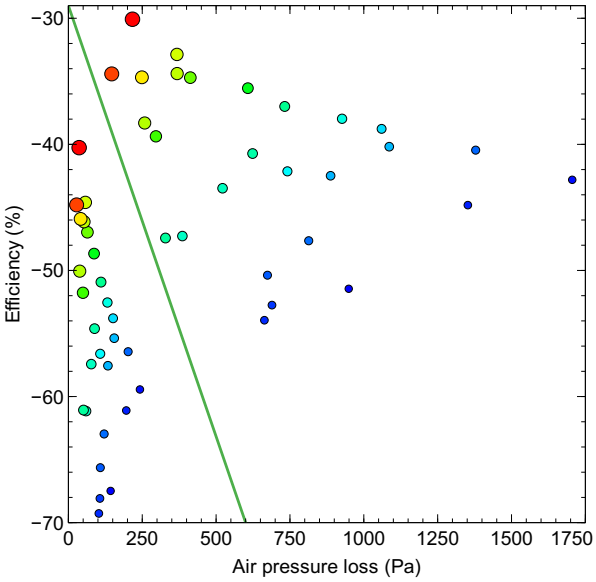

Figure 1: Results in very high and low conditions (points with the same colour and size represent the same geometry and the green line separates the low condition, on the left, from very high condition, on the right)

As the figure 1 shows, points with the same colour and size have the same relative position on both sides of the line, validating the assumption that a solution is optimal in all operating conditions. The very high operating condition was applied in all optimization due to the high spread of the points.

The geometry was changed by applying a scale factor to the height of each channel. It was calculated by $x = \frac{H}{H_{Highland}}$, where $H_{Highland}$ is the height of the original channel and the H is the height given by the genetic algorithm.

4.1.1 Results

The results of the first optimization are presented in the form of a Pareto curve, where the points with '•' belong to the pareto curve.

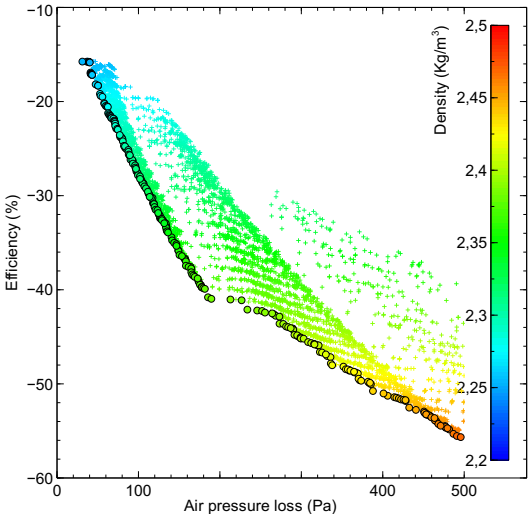

Figure 2: Pareto front varying the density

The figure 2 shows that the density is function of the efficiency and the pressure doesn't have influence due to the low pressure loss.

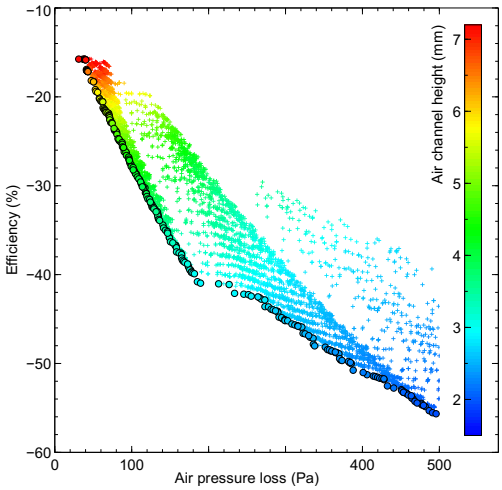

Figure 3: Pareto front varying the air channel height

The height of the air channel is the parameter that varies the most is the efficiency, shown in the figure 3. With the decrease of the channel height, the efficiency increases. The height of the water channels controls the air pressure loss in an indirect way. Keeping constant the height of the air channel and decreasing the height of the water channel, increases the number of channels and consequently decreases the flow velocity.

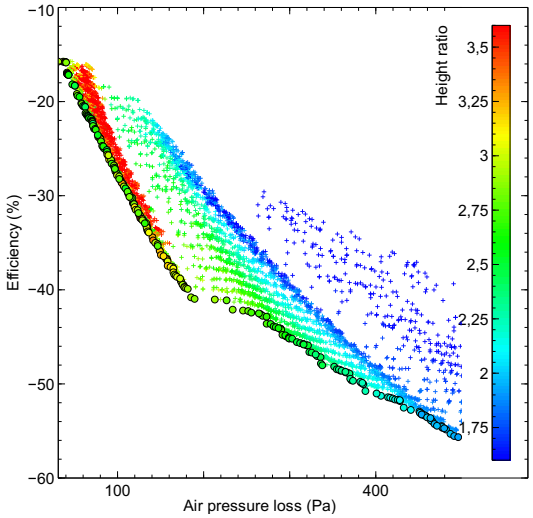

Figure 4: Pareto front varying the height ratio between channels (color scheme limited to values between 1.6 and 3.6)

The figure 4 shows that the solutions that belongs to the Pareto front have a height ratio between 2 and 3, depending on the desired parameter to maximize. If the biggest efficiency is desired, the air channel height must be less than 3.5 mm and the height ratio close to 2. If the lowest pressure drop is desired, the air channel height must be less than 7.2 mm and the height ratio close to 3.

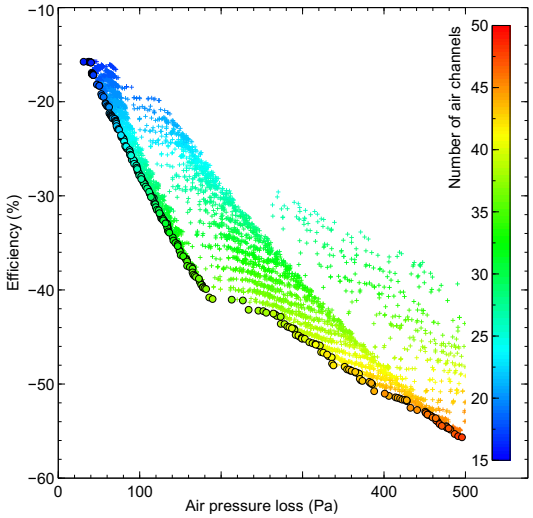

Figure 5: Pareto front variyng the number of channels

Analysing just the number of channels, with the increase in the number of channels, the flow across each channel will decrease. If the UHF condition is assumed, as studied by Islam *et al.* [6], the Dittus-Boelter (4) correlation can be applied. Regarding the Prandlt number of each fluid, the air Prandlt number is 0.7, while the water Prandlt num-

ber is 6. This difference makes the air the limiting fluid in terms of heat transfer, as concluded by Arie *et al*.[1]. In order to increase the heat transfer, the convection coefficient must increase or the air heat capacity ($C = \dot{m}cp$) must decrease. Although with the decrease in the channel height, the flow velocity increases and there is more pressure loss. The figure 5 indicates that with a number of channels higher than 35 and a height ratio smaller than 3, the increase in efficiency is smaller.

The major conclusions taken from this study are:

- There is no solution with higher efficiency and smaller pressure lost than the original geometry;
- The air is the limiting fluid in terms of heat transfer;
- The greater the number of channels, the greater the efficiency and the pressure loss in the air;
- The height ratio must be between 2 and 3;
- The slope on the Pareto front changes around 35 channels and a height ratio of 3;

4.2. Optimization with porous media

The first optimization done allowed to gain some knowledge regarding the trend between the number of channels and the channel height, but no real solution can be obtain in this study because there is no geometry with better performance than the actual geometry with fins. A new study with fins must be done to obtain a solution that can be compared with the actual performance.

To do so, the properties of the *louvered* and *offset* fins were characterized for diferent heights in order to apply the porous media with the thermal non-equilibrium model. The fins porous resistance coefficient, conductivity and heat transfer coefficient were characterized.

4.2.1 Porous resistance coefficients

The porous resistance coefficients were calculated by fitting the results of the simulation for several mass flows across the REV of the fin into the equation (6). Then, the same procedure was done to the fins with different heights, scaling the original mesh to match the desired height. The calculated coefficients were fitted to an equation depending on the scale. The meshes were validated since the results obtained were close to the ones provided by JDeus.

Louvered

Inertial resistance coefficient-*Louvered*

$$K_i = 2.3229 \times 10^{-3} \ln x + 1.8349 \times 10^{-2} \quad (8)$$

Viscous resistance coefficient-*Louvered*

$$K_v = 6.4958 \times 10^{-9} \ln x + 2.2516 \times 10^{-8} \quad (9)$$

Offset

The offset fin has two flow directions, HPD (high pressure drop) and LPD (low pressure drop). The results obtained for different heights, in the HPD direction, indicated that the inertial resistance is independent of the scale used and is equal to 2.4×10^{-4}. The viscous resistance was calculated for different scales and fitted to an equation.

Viscous resistance coefficient-*Offset* HPD

$$K_v = -1.8415 \times 10^{-8} x^2 + \\ +4.8324 \times 10^{-8} x - 5.2 \times 10^{-9} \quad (10)$$

The same study was done to the LPD direction. In this direction, the results obtained for the inertial coefficient were slightly different from the ones provided by JDeus. To correct this difference, the coefficients obtained were multiplied by a factor to fit the coefficients provided by JDeus.

Viscous resistance coefficient-*Offset* LPD

$$K_v = -5.9146 \times 10^{-8} x^2 + \\ +2.3795 \times 10^{-7} x - 4.612 \times 10^{-8} \quad (11)$$

Inertial resistance coefficient-*Offset* HPD

$$K_i = (0.0813x^2 - 0.0761x + 0.0696) \times 0.561497 \quad (12)$$

4.2.2 Thermal conductivity

Since the fins aren't a solid block of aluminium, the conductivity isn't the same in all directions. To achieve another level of reality, the fins were characterized according to their thermal conductivity in different directions. The results were obtained by simulating just the aluminium fin and applying a temperature difference in three different directions. Then the conductivity was calculated by dividing the heat flux and the length in that direction by the area of contact and the temperature difference.

Louvered

For this fin, the scale factor applied made the top and bottom part of the fin thinner and for that reason the results for the y direction (vertical) doesn't follow the trend that the other directions have.

X Direction

$$k_x = 42.96x^{-0.3185} \quad (13)$$

Y Direction

$$k_y = -128.6x^2 + 181.3x + 75.2 \quad (14)$$

Z Direction

$$k_z = 2.916x^{-0.9997} \quad (15)$$

Offset

For this fins, the geometric model used had the same thickness for the different heights.

X Direction

$$k_x = 68.67x^{-1.163} \quad (16)$$

Y Direction

$$k_y = -7.289x^{-0.7056} + 68.71 \tag{17}$$

Z Direction

$$k_z = 57.59x^{-1.218} \tag{18}$$

4.2.3 Heat transfer coefficient

The heat transfer coefficient was calculated by simu-lating a flow between the REV of the fins with a temperature difference applied to the top of the plates. Then, the heat transfer coefficient is calculated by equation (19).

$$h_t = \frac{q}{A \times (T_{alhete} - T_{fluido})} \tag{19}$$

The heat transfer coefficient was calculated for various mass flows and the results were fitted to an equation ($N_u = Re^a_{D_h} P^b_r$) similar to the Dittus-Boelter correlation (4). Then, the a and b coefficients were fitted to an equation dependent on the scale.

Louvered

For this fin, the coefficients were fitted to a Fourier equation (20).

$$\begin{aligned} y(x) = a_0 + a_1 \cos(xw) + b_1 \sin(xw) + \\ + a_2 \cos(2xw) + b_2 \sin(2xw) \end{aligned} \tag{20}$$

The graphs of the fitting are shown in the figures 6 and 7.

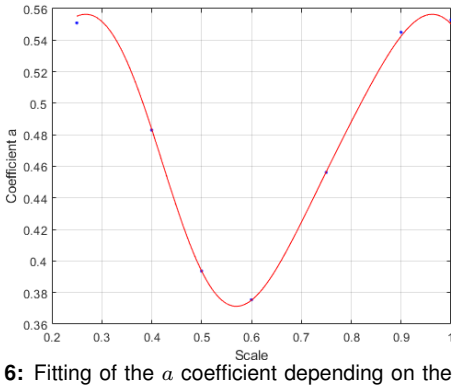

Figure 6: Fitting of the a coefficient depending on the scale - *louvered*

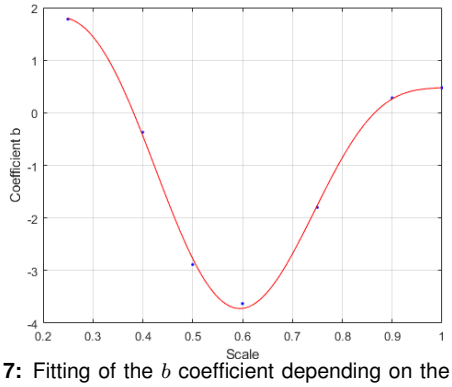

Figure 7: Fitting of the b coefficient depending on the scale - *louvered*

Offset

For this fin, the heat transfer coefficient was evaluated in two directions (HPD and LPD). For the HPD direction, the fitting of the a and b coefficients was done using the equation (20), but for the LPD direction the equation that gave the best fit to the results was a Fourier equation but with less terms, $y(x) = a_0 + a_1 \cos(xw) + b_1 \sin(xw)$.

The graphs of the fitting, for the HPD direction, are shown in the figures 8 and 9, and for the LPD direction, are shown in the figures 10 and 11.

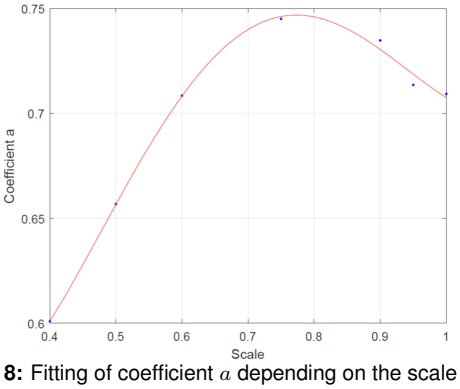

Figure 8: Fitting of coefficient a depending on the scale - HPD

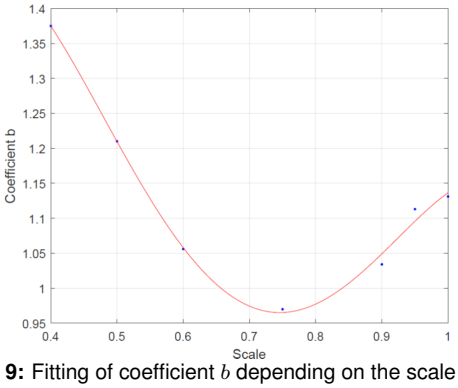

Figure 9: Fitting of coefficient b depending on the scale - HPD

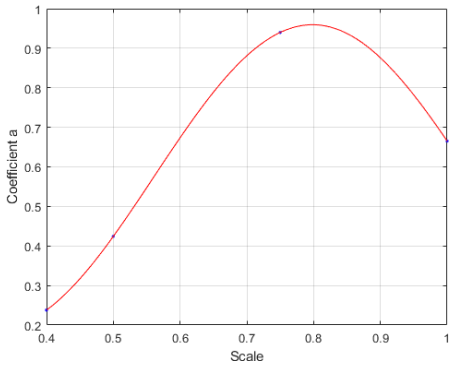

Figure 10: Fitting of coefficient a depending on the scale - LPD

4.2.4 Implementation of the porous media with thermal non-equilibrium model

The porous media was used in a different way that JDeus usually do. They apply the equilibrium

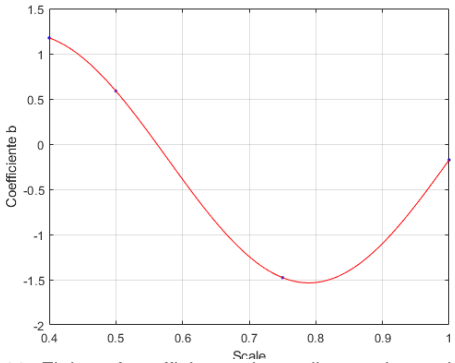

Figure 11: Fitting of coefficient b depending on the scale - LPD

model that solves just one energy equation, assuming that the solid phase and liquid phase have the same temperature. They also correct the differences between the numerical and the experimental results by using a fictitious porosity. They also assume a isotropic thermal conductivity.

In this optimization, the models used were different, starting with the energy model for the porous media. The real porosity was used for both fins too. The turbulence model was also changed since the $k-\omega$ model was validated early in this study. The porosity and the interaction area used for both fins are presented in the table 3.

Table 3: Fins properties

	Louvered	Offset
Porosity	0.9185	0.942
Interaction solid/fluid (/m)	2279.67	961.145

The comparison between this method and the experimental results is presented in the table 4.

Table 4: validation of the results

	$\Delta P_{air}(mbar)$	$\epsilon(\%)$	$\Delta P_{water}(mbar)$	$\rho(kg/m^3)$
2D	57.76	95.93	120.61	3.195
Experimental	56.9	97.7	134.3	3.247

This method had better results than the method used by JDeus. Comparing the tables 2 and 4, the method used in this optimization had results closer to the experimental than the one used by JDeus.

4.2.5 Results from optimization

With this optimization, the results obtained can be compared with the actual performance of the *intercooler* and deliver a concrete solution to improve the actual *intercooler*.

The density is still just a function of the efficiency. The trend seen in the optimization without porous media remains. For better visualization of the results, the parameters in the axis were modified.

The efficiency is still a function of the number of channels. In this case, the optimal results

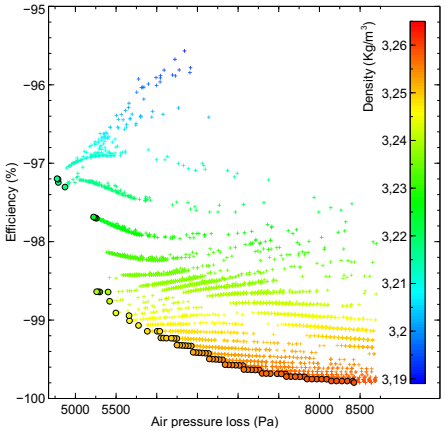

Figure 12: Pareto front varying the outlet air density

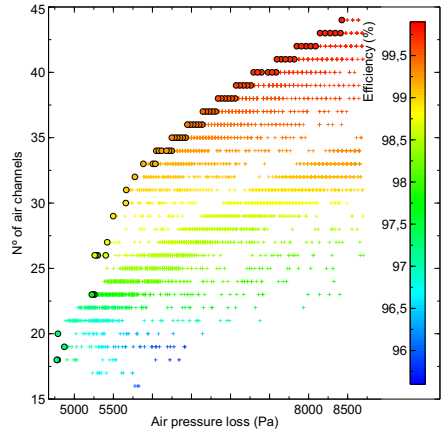

Figure 13: Results variation with the number of channels

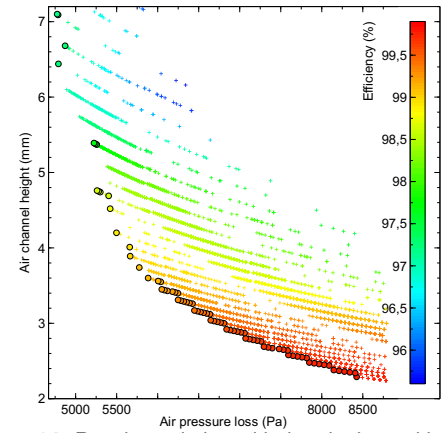

Figure 14: Results variation with the air channel height

were achieved for the maximum air channel height together with the lowest possible water channel height. As shown in the figure 15, the optimal height ratio is between 2.5 and 4 depending on the best parameter desired.

The figure 16 shows the Pareto surface of an optimization with the efficiency, air and water pressure loss as objective parameters. Is easy to understand that the solutions that optimize the air pressure loss and the efficiency are the ones that maximize the water pressure loss.

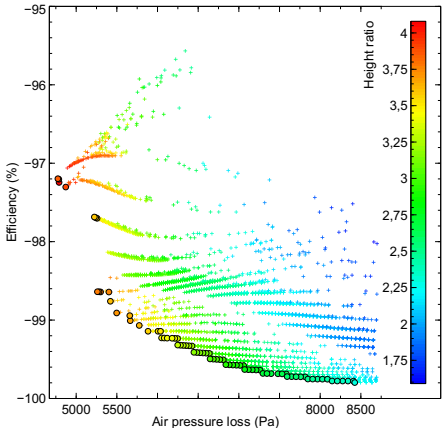

Figure 15: Pareto front varying the height ratio

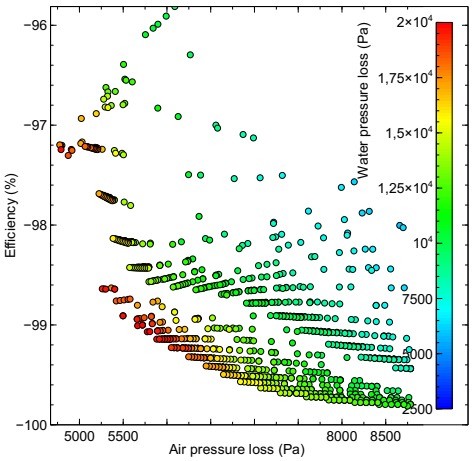

Figure 16: Pareto surface varying ht ΔP_{water}

In the table 5 are the optimal geometries obtained in the optimization that fits the minimal performance demanded by JDeus.

Table 5: Optimal geometries obtained

			Very High			
$H_{air}(mm)$	$H_{water}(mm)$	Nº air channels	$\Delta P_{air}(mbar)$	$\epsilon(\%)$	$\Delta P_{water}(mbar)$	$\rho(kg/m^3)$
2.29	1.00	44	84.25	99.80	120.27	3.259
2.54	1.00	41	78.16	99.72	136.31	3.258
3.61	1.00	33	58.53	99.14	200.79	3.248
4.52	1.50	26	57.94	98.57	137.06	3.239
7.20	2.50	16	57.76	95.93	120.61	3.195

4.2.6 Validation of results with 3D simulation of the complete *intercooler*

The original geometry (Highland) and other two optimized geometries were simulated in a 3D full scale *intercooler* for two different operating points, in order to validate the optimization done. JDeus provided the CAD model for the Highland geometry with a length of 100 mm and the experimental results for this geometry. This size reduction allowed for a smaller mesh size, increasing the simulation speed. The other two geometries simulated (Tetraspis and Nilo) were also 100 mm length. The models used were $k-\omega$ and thermal non-equilibrium.

Highland

The results for this geometry are presented in the table 6. The difference between the 3D results and the experimental results are minimal. The major difference appears in the water pressure loss with a difference of only 4%. The difference of the 2D results are easily justified. Since it simplifies the flow on the channel by assuming pure counter-flow with just axial velocity gradients, the turbulence and pressure loss taken in the intake and exhaust chambers are not simulated. Nevertheless, the 2D model allow to obtain the overall efficiency of the geometry.

Table 6: Results comparison between experimental, 2D and 3D full scale model

	Very High			Low		
	$\epsilon(\%)$	$\Delta P_{air}(mbar)$	$\Delta P_{water}(mbar)$	$\epsilon(\%)$	ΔP_{air}	ΔP_{water}
EXPERIMENTAL	84.40	50.00	100.00	96.60	11.40	28.00
2D	83.75	36.01	68.92	97.73	8.36	18.96
3D REAL	84.09	48.06	96.06	97.30	10.28	26.21

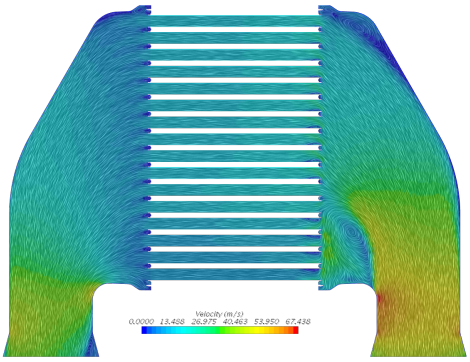

Figure 17: Air velocity profile - *Highland*

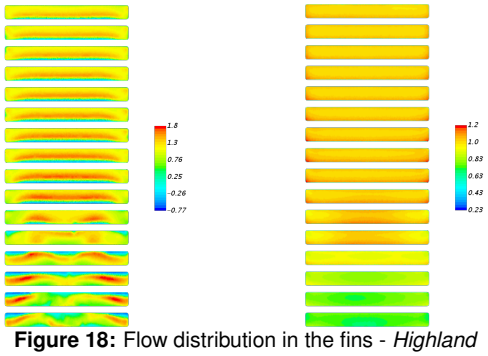

Figure 18: Flow distribution in the fins - *Highland*

As the figure 17 shows, the intake chambers have a recirculation zone near the bottom channels of the core. The expansion of the chambers that happens after the inlet creates an adverse pressure gradient and a vortex is generated. This vortex is the reason why it doesn't have a uniform flow across all channels, as the figure 18 shows.

Tetraspis

This geometry has 41 air channels with an height of 2.54 mm and 42 water channels with a height of 1 mm.

Table 7: Results comparison between 2D and 3D.

	Very High			Low		
	$\epsilon(\%)$	$\Delta\mathbf{P_{air}(mbar)}$	$\Delta\mathbf{P_{water}(mbar)}$	$\epsilon(\%)$	$\Delta\mathbf{P_{air}}$	$\Delta\mathbf{P_{water}}$
2D	96.91	47.60	78.18	99.92	12.04	23.55
3D	97.67	63.64	117.38	100.00	15.85	36.83

The major differences between the 2D and the 3D are still the pressure losses in both fluids. Once again, the efficiency can be obtained using the 2D model because the difference to the 3D model is less than 1%.

Nilo

This geometry has 26 air channels with a height of 4.52 mm and 27 water channels with a height of 1.5 mm.

Table 8: Results comparison between 2D and 3D.

	Very High			Low		
	$\epsilon(\%)$	$\Delta\mathbf{P_{air}(mbar)}$	$\Delta\mathbf{P_{water}(mbar)}$	$\epsilon(\%)$	$\Delta\mathbf{P_{air}}$	$\Delta\mathbf{P_{water}}$
2D	93.22	35.77	78.43	99.73	8.71	22.31
3D	93.03	52.86	97.72	99.64	12.58	26.67

The differences between results remain the same seen in the other two geometries.

4.2.7 $k-\epsilon$ Turbulence model

Since JDeus uses the $k-\epsilon$ model, a comparison between the results obtained using thermal non-equilibrium model together this model and with $k-\omega$ must be done to realize if the JDeus method is better than the one applied in the optimization. The results of the 3D full scale *intercooler* are in the table 9.

Table 9: Results comparison between turbulence models

	$\epsilon(\%)$	$\Delta\mathbf{P_{air}(mbar)}$	$\Delta\mathbf{P_{water}(mbar)}$
$k-\omega$	84.09	48.06	96.06
$k-\epsilon$	86.21	46.03	97.56
Experimental	84.40	50.00	100.00

The results of the $k-\epsilon$ are far from the experimental than the results of the $k-\omega$. The efficiency is 2% higher than the experimental and the pressure loss in the air have a 4 mbar difference. The model $k-\omega$ is better to replicate the flow inside the *intercooler* than the $k-\epsilon$.

4.2.8 Optimization for volume reduction

The results obtained in the optimization with porous media showed that the efficiency is near the 100%. This indicates that the *intercooler* is oversized since one parameter is near the maximum value possible. An optimization for volume reduction was made to try to reach the best geometry not only for performance but also for the lowest volume possible. Like the previous optimizations, an initial optimization without porous media was done and then the porous media was applied.

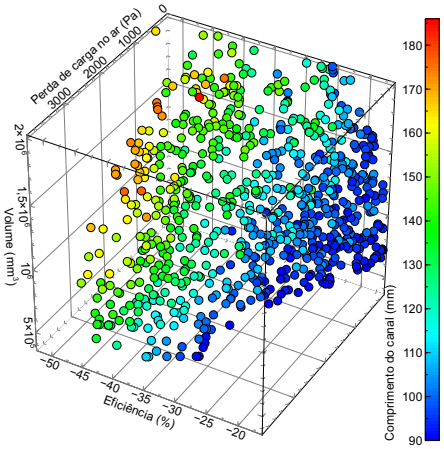

Figure 19: Pareto surface - channel length

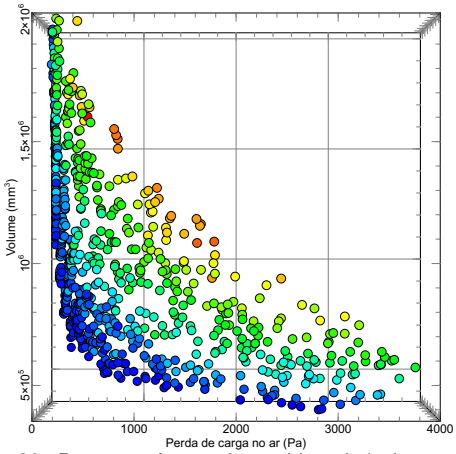

Figure 20: Pareto surface - channel length (volume and pressure loss)

No porous media

The channel length is a crucial parameter in the performance of the *intercooler*. With the decrease in the channel length, the pressure loss and the efficiency decrease, making it possible to decrease the height ratio in order to increase the efficiency.

With porous media

With fins, the decreasing of the channel length is the best way of reducing the core volume. The same conclusion in the optimization without fins applies to the optimization with fins.

5. Conclusions

The method used for optimization, substituting the 3D model by a 2D model, is valid and can replace the full scale study of an *intercooler*, regarding the efficiency performance. This method also decreases the simulation time from 1-2 days to 1-3 minutes. The $k-\omega$ model and the thermal non-equilibrium model provide better results than the method used by JDeus. The optimizations done provided several solutions that are better in terms of efficiency than the actual geometry in production by JDeus. Also, solutions with smaller volume (al-

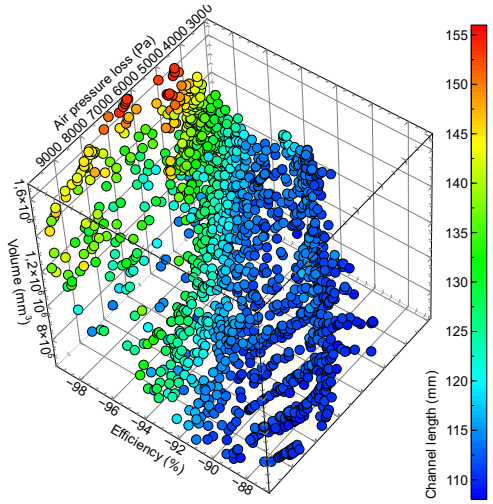

Figure 21: Pareto surface - channel length

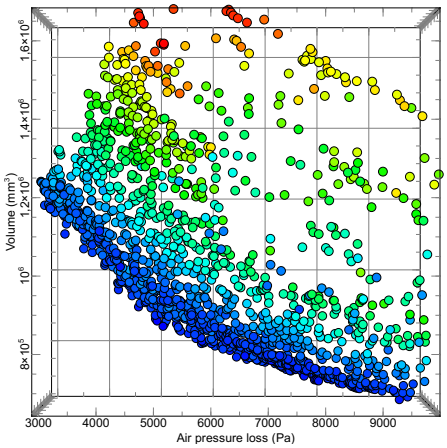

Figure 22: Pareto surface - channel length (volume and pressure loss)

most 50% of the original volume) and better results in terms of efficiency were found.

The method created can be used to optimize every type of heat exchanger and is flexible enough to change the fins used, although the fins properties must be known.

References

[1] M. Arie, A. Shooshtari, R. Tiwari, S. Dessiatoun, M. Ohadi, and J. Pearce. Experimental characterization of heat transfer in an additively manufactured polymer heat exchanger. *Applied Thermal Engineering*, 113, 11 2016.

[2] S. Bailey, M. Egerer, M. Hultmark, and A. Smits. Estimating the value of von karman's constant in turbulent pipe flow. *Journal of Fluid Mechanics*, 749:79–98, 06 2014.

[3] E. Canli, S. Darici, and M. Ozgoren. Intercooler effect on conventional supercharging systems. 11 2010.

[4] F. W. Dittus and L. M. K. Boelter. *Heat transfer in automobile radiators of the tubular type*. The University of California Publications on Engineering, 2 edition, 1930.

[5] V. Gnielinski. New equations for heat and mass transfer in turbulent pipe and channel flow. *Int. Chem. Eng*, 16(2):359–368, 1976.

[6] M. Islam, N. Wijeysundera, and J. Ho. Heat and mass transfer effectiveness and correlations for counter-flow absorbers. *International Journal of Heat and Mass Transfer*, 49:4171–4182, 10 2006.

[7] T. Kim. Development of friction model for offset strip fin with separated viscous and inertial resistances. *Journal of Mechanical Science and Technology*, 31:6051–6057, 12 2017.

[8] T. Kim, H.-C. Kang, and J. Lee. A porosity model for flow resistance calculation of heat exchanger with louvered fins. *Journal of Mechanical Science and Technology*, 30:1943–1948, 04 2016.

[9] W. Lin and B. Sunden. Vehicle cooling systems for reducing fuel consumption and carbon dioxide: Literature survey. *SAE Technical Papers*, 05 2010.

[10] S. Sutera and R. Skalak. The history of poiseuille's law. *Annual Review of Fluid Mechanics*, 25:1–20, 11 2003.

[11] G. Xie, B. Sunden, and Q. Wang. Optimization of compact heat exchangers by a genetic algorithm. *Applied Thermal Engineering*, 28:895–906, 06 2008.

[12] İsmail Çagatay Koyuncuoglu. Optimization of air to air cross flow heat exchanger. Master's thesis, Middle East Technical University, 2018.